

INTRAOPERATIVE OPTICAL COHERENCE TOMOGRAPHY (OCT) GUIDANCE OF VITREORETINAL SURGERY

Hesham Gabr^{1,2}, Sherif Zaki Mansour¹, Sherif Nabil Embabi¹,
Tamer H. Mahmoud^{2,4}, and Cynthia A. Toth^{2,3},

ABSTRACT:

¹ Department of Ophthalmology,
Ain shams University, Cairo,
Egypt.

² Department of Ophthalmology,
Duke University Medical Center,
Durham, NC, United States

³ Department of Biomedical
Engineering, Duke University,
Durham, NC, United States.

⁴ Department of Ophthalmology
Oakland University, William
Beaumont Hospital, Michigan
USA

Corresponding Author:
Hesham Gabr

Mobile [209194505888](tel:209194505888).

E-mail:
hesham.gabr@duke.edu.

Received :1/6/2020

Accepted: 25/6/2020

Online ISSN: 2735-3540

Background: Multiple studies have described the utility of intraoperative spectral-domain OCT (SD-OCT) with two dimensional (2D) B-scan imaging in the management of numerous vitreoretinal disorders including macular holes, vitreomacular traction disorders, epiretinal membranes and retinal detachment. Some of these studies also described post-processing of the 2D B-scans to obtain 3D images. With the advancement of intraoperative OCT technology, live volumetric (4D, i.e. 3D over time) visualization of different anterior and posterior segment surgeries has been described in recent studies using intraoperative swept-source microscope-integrated OCT (SS-MIOCT). Our study aims to explore the potential utility of SS-MIOCT during vitrectomy for complications of proliferative diabetic retinopathy.

Aim of the work: To evaluate the use of live volumetric (4D) intraoperative swept-source microscope-integrated OCT (SS-MIOCT) in vitrectomy for proliferative diabetic retinopathy (PDR) complications.

Patient and Methods: In this prospective study, we analyzed a subgroup of cases with PDR complications that required vitrectomy and that were imaged by the research SS-MIOCT system. In near real time, images were displayed in stereo heads-up display facilitating intraoperative surgeon feedback. Postoperative review included scoring image quality, identifying different diabetic retinopathy (DR)-associated pathologies and reviewing the intraoperatively documented surgeon feedback.

Results: Twenty eyes were included. Indications for vitrectomy were tractional retinal detachment (TRD, 16 eyes), combined tractional-rhegmatogenous retinal detachment (2 eyes) and vitreous hemorrhage (2 eyes). Useful, good quality 2D (B-scans) and 4D images were obtained in 16/20 eyes (80%). In these eyes, multiple DR pathologies could be imaged. SS-MIOCT provided surgical guidance, e.g. in identifying dissection planes under fibrovascular membranes, and in determining residual membranes and traction that would benefit from additional peeling. In 4/20 eyes (20%) acceptable images were captured, but they were not useful due to high TRD elevation which was challenging for imaging.

Conclusion: SS-MIOCT can provide important guidance during surgery for PDR complications through intraoperative identification of different pathologies and facilitation of intraoperative decision making.

Key words: Diabetic retinopathy; 4D intraoperative OCT; swept-source intraoperative microscope integrated OCT; Live volumetric

intraoperative microscope integrated OCT; Proliferative diabetic retinopathy; Tractional retinal detachment; Vitreous hemorrhage.

INTRODUCTION:

Visual impairment in diabetic retinopathy is largely due to macular edema, ischemic maculopathy and/or complications of proliferative diabetic retinopathy (PDR). The main complications of PDR include vitreous hemorrhage, tractional retinal detachment (TRD) and combined tractional rhegmatogenous retinal detachment¹. These complications have been treated with increasingly successful outcomes with the advances introduced into vitreoretinal surgery². One recent advance is the integration of optical coherence tomography (OCT) into the operating microscope to provide high resolution imaging feedback to the surgeons during surgical maneuvers.³ While preoperative OCT is often used in surgical planning for diabetic surgery, preoperative assessment of the retina is not possible with OCT in eyes with dense vitreous hemorrhage, high TRD, or combined tractional-rhegmatogenous retinal detachment (TRD-RRD). In these cases, ultrasound plays an important role in preoperative assessment of the retinal macro architecture by detecting the presence and extent of retinal detachment.^{4,5} Despite this important role for ultrasound, preoperative evaluation remains deficient as it lacks important information about the micro architecture of the retinal layers which is of particular importance in diabetic cases.⁶

Recent studies have described the utility of intraoperative spectral-domain OCT (SD-OCT) with two dimensional (2D) B-scan imaging in the management of numerous vitreoretinal disorders including macular holes, vitreomacular traction disorders, epiretinal membranes and retinal detachment.⁷⁻¹⁵ Some of these studies^{7,12} also described post-processing of the 2D B-scans to obtain 3D images. With the advancement of intraoperative OCT technology, live

volumetric (4D, i.e. 3D over time) visualization of different anterior and posterior segment surgeries has been described in recent studies using intraoperative swept-source microscope-integrated OCT (SS-MIOCT).^{16,17} Our study aims to explore the potential utility of SS-MIOCT during vitrectomy for complications of PDR.

PATIENTS AND METHODS:

Study design and enrollment:

This is a prospective, single center multi-surgeon study on the use of SS-MIOCT during vitrectomy for PDR complications. This study is a part of a prospective clinical study of intraoperative OCT use in ophthalmic surgery, which was approved by the Duke University Health System Institutional Review Board and was conducted in accordance with the Declaration of Helsinki. All patients gave written informed consent to be part of this study before enrollment. The study is registered on ClinicalTrials.gov with study number NCT01588041.

Inclusion criteria for this analysis were patients with a diagnosis of PDR who consented to participate in the prospective MIOCT study from January 2015 to March 2017. Twenty patients (8 males and 12 females) in the larger study database met the inclusion criteria. The average age was 45.3 years (range: 26-75 years). The cases included 16 cases with TRD involving or threatening the macula, 2 cases with TRD-RRD and 2 cases with dense non-clearing vitreous hemorrhage.

Surgical procedure and intraoperative OCT imaging:

Standard 3-port pars plana vitrectomy was performed with either 23 or 25-gauge instrumentation using the Constellation

vitrectomy machine (Alcon Laboratories Inc., Ft. Worth, TX). An additional 4th port for chandelier lighting was used in 4 cases to allow for bimanual surgical maneuvers. Cases were imaged using SS-MIOCT capable of producing live volumetric (4D) imaging during surgical maneuvers.¹⁷ Retinal imaging was performed either through a disposable flat contact lens or a non-contact wide-field viewing system depending on the surgeon's preference. Images were captured before, during and after different surgical steps. To provide immediate 2D and 4D MIOCT visualization to the surgeon with surgeon control of the volumetric rendering perspective, we utilized a heads-up display (HUD) integrated into the operating microscope. A foot-operated joystick allowed the surgeon to change the rendering orientation of the SS-MIOCT volumes projected with the HUD while performing the surgery. The volumes were commonly positioned with 20-30 degree downward tilt at the front of the volume for surface work. For subsurface surgery, this was pivotal during maneuvers to gain from different perspectives. The HUD projected the 3D volume and selected B-scan in the periphery of the view within the surgical oculars^{17,18}. This feature allowed the surgeon to visualize the surgical field with an adjustable 3D visual perspective in addition to the 2D B-scan.¹⁸ The surgeon used this information for live guidance of surgical maneuvers. Surgeon feedback was documented intraoperatively using a standardized case report form that included comments on the surgical step, instruments used and image quality. The use of SS-MIOCT to guide surgical steps and facilitate intraoperative decision making was documented in the postoperative notes.

Intraoperative OCT imaging protocol¹⁷:

For intraoperative OCT imaging, we used a 5 × 5 mm field of view. The volumetric frame rate varied between 1–10 volumes per second by varying the number

of A-lines per volume to determine the fastest volume rate that would still allow adequate lateral resolution. The most common scan parameters selected were 300 A-lines/B-scan and 100 B-scans/volume, which resulted in a volume rate of 3.33 Hz.

Image review and analysis:

Postoperative review included scoring image quality, reviewing the surgeon feedback on intraoperative visualization, identifying different pathologies associated with diabetic retinopathy and tracking surgical maneuvers. Image quality was scored as “good” if the retina was clearly visualized in 2D (B-scans) and 4D images. In areas of the retina with overlying fibrovascular membranes, image quality was scored as “good” if the retina could be distinguished from the overlying membranes in the 2D (B-scans) and 4D images. From each surgery, the visualization of different pathologies were recorded and tabulated along with the use of SS-MIOCT in demonstrating surface and sub-surface pathologies prior to and during maneuvers. Video clips and still images were selected to illustrate the findings.

RESULTS:

Identification of diabetic retinopathy-related pathologies:

Of the 20 eyes imaged, good quality 2D (B-scans) and 4D images were obtained in 16 eyes. These cases were: 12 cases with TRD, 2 cases with TRD-RRD and 2 cases with vitreous hemorrhage imaged after clearing the hemorrhage. In the remaining 4 cases with TRD, the images were classified as poor quality, because although the image quality was acceptable (Fig. 1), the complex tissue and the elevation of a very high TRD appeared to present a challenge to differentiating tissues from retina across the limited depth of field of the SS-MIOCT system.

Identification of different pathologies associated with diabetic retinopathy was feasible in all cases with good quality images. In multiple cases, more than one pathology or structure could be identified.

Table 1 and figures 1-6 summarize the differences between 2D (B-scan) and 3D/4D images in visualization of pathologies and structures.

Table 1: Visualization of structures in 2D and 3D/4D images.

| Pathology/Structure (# of eyes: case #s) | 2D (B-scan) image | 3D/4D image | Figures /Videos |
|---|---|--|--------------------|
| Preretinal fibrovascular tissue 14 eyes (TRD & TRD-RRD) Case #: 1-3, 5, 9, 11- 14, 16-20) | 2D scans differentiated these fibrovascular tissues from the underlying retina but it was difficult to appreciate the full morphology of the membrane in relation to the retina. | Image enabled the surgeon to visualize the tractional fibrovascular membrane and distinguish it from the underlying retina. It also facilitated the visualization of the complete configuration of the membrane in relation to the retina. | N/A |
| Preretinal fibrovascular tissue (4 eyes , visible over high TRD) Case #: 4, 6, 7, 15) | Configuration was complex and the fibrovascular tissue could not be distinguished from the retina. | Fibrovascular tissue could not be distinguished from retina, although areas extending upward and suggestions of retinal elevation were visible. | Fig.1 |
| Tractional schisis (3 eyes:11, 14, 17) | Images showed the subsurface columnar retinal tissues characteristic of retinoschisis. The thickness of each column cannot be appreciated due to the cut through the tissues. | Images also showed the subsurface columnar tissues characteristic of retinoschisis. We could appreciate the full configuration of these multiple columnar tissues and the schitic cavities in between. | Fig.2 |
| Subretinal fluid (9 eyes: 1, 2, 8, 9, 13, 14, 18-20) | 2D and 3D scans showed the subretinal optically empty space indicating the presence of subretinal fluid under the elevated deep retinal layers. | | Fig.3 |
| Intraretinal fluid (3 eyes: 3, 8 , 14) | B-scans clearly showed the optically empty spaces within the retinal layers indicating intraretinal fluid. | 3D image showed the effect of intraretinal fluid on the arrangement of structures of the retina. | Fig.3 |
| Focal retinal traction (6 eyes: 5, 9, 11, 13, 14, 20) | One could appreciate the focal points of traction. Although B-scan showed the number of traction points across many B- scans, it did not show the whole area of interest in a single image. | One could appreciate the number and configuration of the focal points of traction across an area of interest in a single image. Also, volume rotation allowed for viewing these points from different perspectives. | Fig.4 |
| Broad traction (5 eyes: 1, 9, 14, 16, 17) | While some of the 2D scans clearly showed the broad areas of traction, some of the 2D scans did not reveal the whole area of broad traction. | 3D image provided more comprehensive anatomical details about the broad traction areas through images encompassing the whole area of interest. Again, volume rotation (even partial) allowed for better understanding of the configuration of these broad areas of traction. | Fig.4 |
| Laser scars (3 eyes: 3, 11, 17) | These areas showed retinal atrophy and adhesion bridging between choroid and detached retina. The thickness and pattern of these bridges (like the columnar tissues mentioned in schisis) cannot be appreciated due to the cut through the tissues. | Using 3D imaging and volume rotation, one can see the relation of these scars to the adjacent retina which could not be detected through B-scans. | Fig.5 |
| Secondary ERM (5 eyes: 3, 9 , 12, 14, 18) | In both scans, ERMs appeared as fine membranes over the retina and were different from the thick fibrovascular diabetic membranes that can induce TRD. | | N/A |

| | | | |
|---|---|--|-------|
| Full thickness retinal hole (1 eye: 8) | Small full thickness retinal hole inferior to the fovea was detected. | Due to the small size of the hole, resolution of the 3D image did not allow for clear visualization of the hole. | Fig.6 |
| Dexamethasone intravitreal implant (Ozurdex; Allergan Inc, Irvine, CA) (1 eye: 1) | Image showed the cross section of the implant. | The implant movement during tissue manipulation was better detected on the 4D images | N/A |

Intraoperative guidance of surgical steps and intraoperative decision making:

SS-MIOCT provided guidance and useful information to intraoperative decision making especially in the following situations: after removal of dense vitreous hemorrhage, to determine tissue planes and full thickness dissection of fibrovascular membranes, and to evaluate the necessity for further membrane peeling.

For the 2 cases with vitreous hemorrhage, after clearing the blood, SS-MIOCT revealed the extent of macular distortion from an epiretinal membrane (ERM). In one of these cases, after ERM and internal limiting membrane peeling, a small full thickness hole inferior to the fovea was detected by SS-MIOCT through examination of 2D B-scans across the site of the hole(Figure6).Decision was made to leave the eye filled with 20% SF6 as a tamponade agent to aid closure of the detected retinal break.In the other case with vitreous hemorrhage, SS-MIOCTof the posterior pole showed an attached macula with ERM superior to the fovea with preserved foveal contour. Based on these findings, decision was made not to peel the membrane and gas tamponade was not used.

During dissection of proliferative fibrovascular membranes, SS-MIOCT with HUD enabled the surgeon to view the interaction between the instruments and the retina/ preretinal membranes in near real-time volumetric motion in all cases that had good quality images while the HUD was in use (11 out of the 20 cases). This included peeling tissue off the retinal and optic nerve head surface and excision of tissue by the vitreous cutter (whose tip shows up as twin

reflective spots)and scissors. SS-MIOCT also permitted the surgeon to accurately assess the distance of the instruments from the surface of the tissue of interest. Due to the ability of surgeon-controlled volume rotation, the surgeon was able to view the interaction of the instruments with the preretinal membranes in different angles.

In 2 cases with TRD, delamination was initiated after viscodissection, which was achieved by creating a hole in the dense, broad fibrovascular membrane and injecting viscoelastic. In one of these cases, only through the SS-MIOCT imaging in both 2D B-scans and 4D, the surgeon could detect that viscodissection was not achieved because there was a partial thickness hole created in the membrane rather than the desired full thickness hole. The membrane opening was revised to full thickness, under SS-MIOCT guidance, facilitating successful viscodissection. By rotating the volume, the surgeon could visualize the space filled with viscoelastic, the inner surface of the underlying retina, the hole in the fibrovascular tissue and the excision of fibrovascular tissue with the vitreous cutter from either above or from the undersurface of the fibrovascular membrane (Fig.7)

SS-MIOCT feedback also facilitated decision making for further membrane peeling. In one case with TRD, perfluorocarbon (PFC) liquid was infused after membrane peeling was deemed sufficient to determine if retina was able to lie flat at the posterior pole. No residual subretinal fluid was observed on SS-MIOCT. Decision was then made to perform fluid-air exchange without additional peeling of membranes. In another case with TRD,

SS-MIOCT showed vitreomacular traction with a large central intraretinal macular cyst. Upon relief of vitreomacular traction, unroofing of the cyst was noted on SS-MIOCT without evidence of macular hole (Fig. 8). Thus, decision was made not to perform further release of the vitreomacular adhesions.

Artifacts that affected our static and dynamic images:

Various artifacts that could impact OCT B-scan and volume quality were encountered during the study. These artifacts included distortion of the volumes due to motion, hyper-reflective artifacts due to undesired reflections from optical components in the system, and hypo-reflective artifacts such as shadowing. Shadowing artifacts often resulted from strong reflections from metallic instruments located over the retina or absorption of OCT light in blood. Variations of these shadowing artifacts, however, were also present in the conventional surgical view. For example, the presence of blood or surgical instruments could also obscure the surgeon's visualization of underlying retinal tissue through the microscope. Additional hypo-reflective artifacts could also arise from poor alignment of the OCT beam through the patient's pupil that would result in images with poor contrast. Hyper-reflective artifacts arose due to strong undesired reflections of the OCT light from commercial optical components with anti-reflective coatings not suitable for near-infrared light. These artifacts appeared in B-scans and volumes as bright structures with unique contours that could be readily distinguished from tissue (see Fig.7 A2, B2 and F1 for example). Moreover, the instruments used in this study were commercially available and not optimized for OCT visibility. As a result, the visibility of some instruments on OCT was

limited, such as the vitreous cutter for which only the tip was visible on OCT.

Outcomes after SS-MIOCT surgery:

Of the 14 cases with good SS-MOICT image quality and retinal detachment (the 4 cases with poor image quality were excluded from further analysis), 13 were successfully attached in the early postoperative period and one case had a rhegmatogenous retinal detachment at 2 weeks after surgery due to a peripheral retinal break. In the late postoperative period, one case showed recurrent retinal detachment after 4 months due to proliferative vitreoretinopathy under silicone oil and the retina was reattached after a reoperation. Another case showed a retinal fold nasal to the fovea which was released at the time of silicone oil removal 5 months after the first surgery. The two cases with dense vitreous hemorrhage (with no retinal detachment) had no recurrent postoperative hemorrhage.

We were also able to capture good quality OCT images of the macula in early (within 1 month) and late postoperative period except for 2 cases that did not have early postoperative OCT and late postoperative visits. The early postoperative OCT confirmed macular attachment in 13 cases, although in one of these cases, OCT showed minimal microscopic subretinal fluid while it appeared to be clinically attached. This subretinal fluid resolved on further follow ups. In another case, OCT confirmed a full thickness retinal fold nasal to the fovea which was surgically released later (as discussed before). Related to the severity of DR, most of eyes showed (either separately or in combination) edema, intraretinal cysts, inner retinal irregularities, residual retinal traction and retinal thinning. Late postoperative OCT (after the first month) showed gradual improvement of retinal contour in most cases.

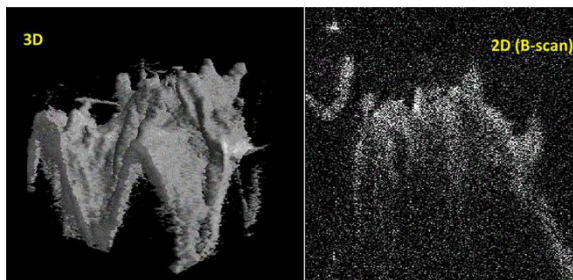


Fig.1: An example of a case with poor image quality. Due to complexity of pathology and high tractional retinal detachment, intraoperative swept-source microscope-integrated OCT could not distinguish the retina from the fibrovascular membranes in 2D and 3D images.

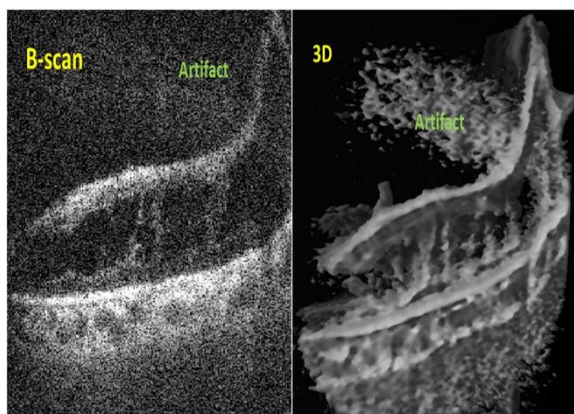


Fig.2: Intraoperative swept-source microscope-integrated OCT shows retinoschisis. B-scan (2D) and 3D images show the subsurface columnar retinal tissues characteristic of retinoschisis.

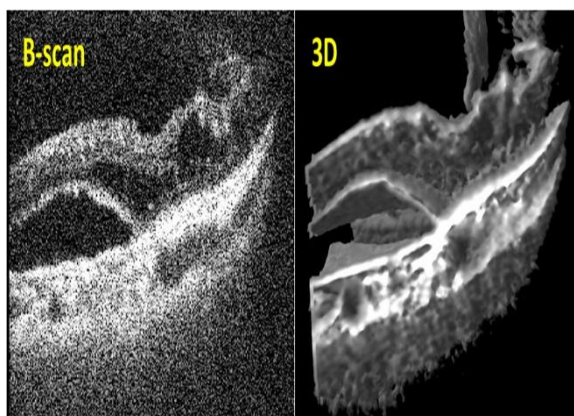


Fig. 3 : Intraoperative swept-source microscope-integrated OCT shows subretinal and intraretinal fluid in 2D (B-scan) and 3D images

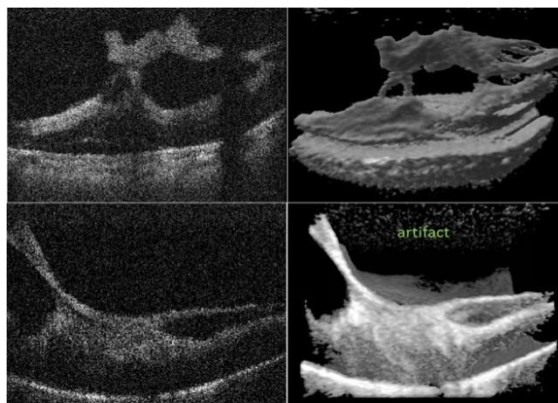


Fig. 4: Intraoperative swept-source microscope-integrated OCT shows focal versus broad attachment of the fibrovascular membrane to the retina. Above row: B-scan (2D) and 3D images of focal membrane attachment. Below row: B-scan (2D) and 3D images of broad membrane attachment

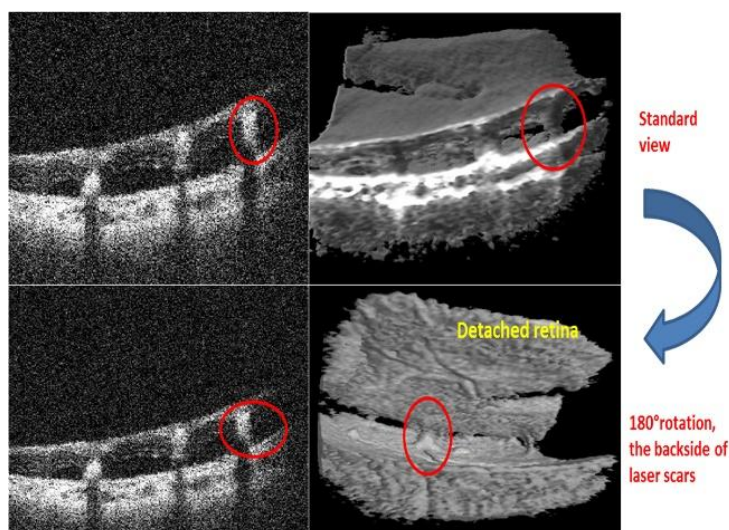


Fig. 5: Intraoperative swept-source microscope-integrated OCT shows laser scars as adhesions bridging choroid to detached retina (red circles). While the B-scans (left column) look the same, the 3D images (right column) show the spatial configuration of the laser scars from 2 different angles (through volume rotation) in relation to the detached retina.

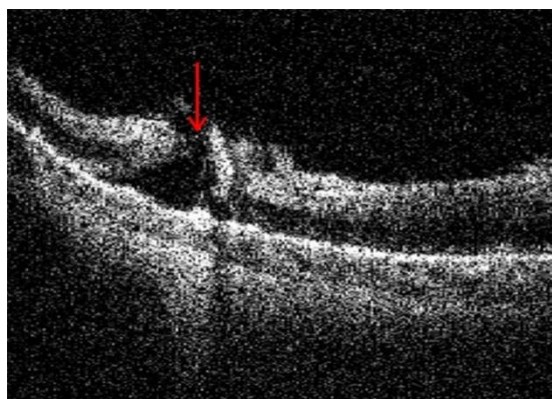


Fig.6: B-scan from Intraoperative swept-source microscope-integrated OCT shows small full thickness hole (arrow) detected inferior to the fovea with minimal residual membranes at the edges of the hole.

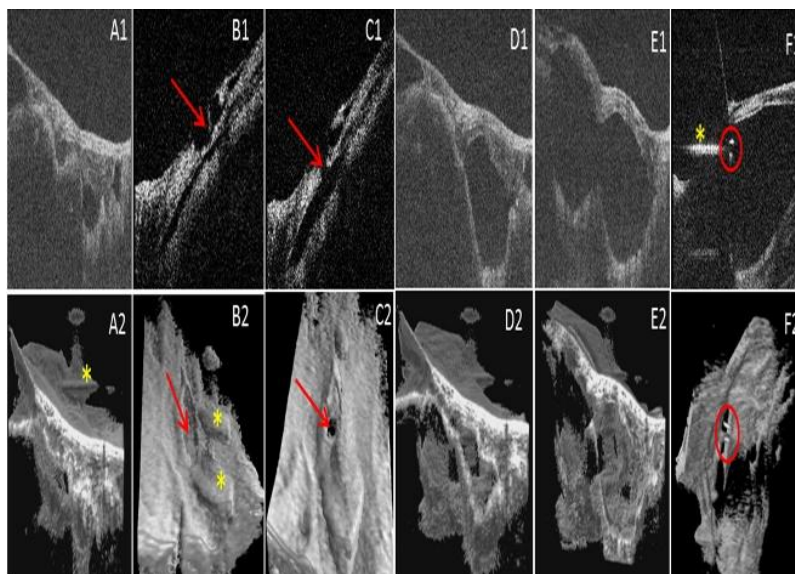


Fig.7: Intraoperative swept-source microscope-integrated OCT guidance of viscodissection of a tightly adherent fibrovascular membrane. Above row: B-scans, below row: 3D images. A1,2) Images show the membrane overlying the retina. B1,2) Images show an initial partial thickness hole (arrow) created in the membrane which did not allow for viscoelastic injection. C1,2) Images show the hole (arrow) after being converted to full thickness allowing viscoelastic injection. D1,2) Starting dissection of the membrane from the retina as the viscoelastic being injected. E1,2) Progression of the membrane dissection from the retina with more viscoelastic injection and more space created between the retina and the membrane. F1) Vitrectomy cutter tip (circle) going through the hole in the space created by viscoelastic to interact with membrane. F2) Hole and cutter tip (circle) as visualized from the under surface of the membrane with the help of volume rotation. A2, B2, F1: Artifacts(*)

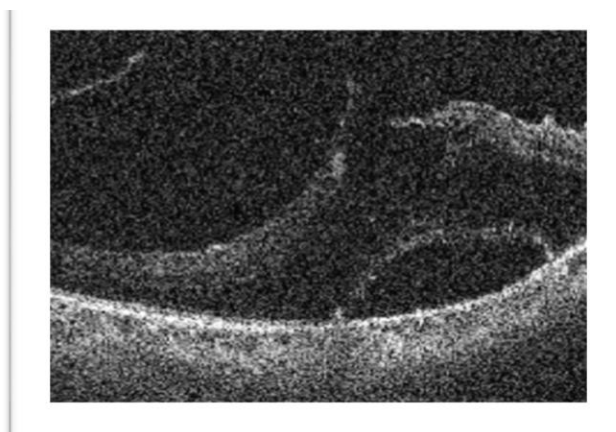


Fig.8: B-scan from intraoperative swept-source microscope-integrated OCT shows deroofed macular cyst noted during release of vitreomacular traction.

DISCUSSION

In 2008, Iwasaki T et al¹⁹ described the use of Fourier-domain OCT (Topcon 3D-1000, Topcon, Tokyo, Japan) in clinic to obtain a 3D image of a diabetic fibrovascular membrane showing the underlying adhesions to the retina. The authors

concluded that 3D visualization of a fibrovascular membrane is an effective tool for understanding the 3D structure of the membrane and can provide the surgeons preoperatively with important information such as the location of epicenters which is useful for safe membrane dissection. In

2009, Dayani et al²⁰ brought this information into the operating room using handheld SD-OCT at pauses in surgery for 8 posterior segment cases including 2PDR cases to show removal of ERM and release of tractional attachments. In 2015, Ehlers et al²¹ discussed the role of a microscope-mounted handheld intraoperative SD-OCT to image the retina at pauses during surgery in 23 cases with vitreous hemorrhage due to different etiologies including 19 PDR cases. The authors showed that 87% of cases had retinal pathologies in the form of macular edema, ERM or retinal detachment, and concluded that intraoperative detection of these pathologies impacted intraoperative and postoperative decision making. In 2015, using a microscope-integrated SD-OCT in 12 PDR cases, Ehlers et al¹⁰ described the role of viewing 2D (B-scan) intraoperative OCT images for identifying surgical planes during membranes dissection. In 2016, Carrasco-Zevallos OM et al¹⁷ described the use of the current SS-MIOCT system in 48 eyes that underwent different anterior and posterior segment surgeries and concluded that this technology could alter the surgeon's decision-making to optimize surgical outcomes. Our report further advances this progression of intraoperative OCT imaging by addressing the use of this system in diabetic vitreoretinal surgery through both 2D (B-scans) and 4D capture with the surgeon using a HUD to view the images within the microscope oculars in surgeries for PDR complications.

We first addressed the viewing of retinal morphology and pathologic structures in these cases with PDR complications. In addition to the identification of the typical diabetic fibrovascular membranes in 14 of the 18 cases with proliferative tissue (and in four additional cases in which membrane was visible but could not be distinguished from the steep detached retina), SS-MIOCT enabled visualization of 3D anatomic relationships in a broad range of other diabetic retinopathy-related pathologies such

as tractional retinoschisis versus tractional retinal detachment, focal versus broad retinal traction, and intraretinal versus subretinal fluid. While the 2D (B-scans) images could be sufficient for simple pathologies like ERM and macular hole, this is not the case with complex diabetic pathologic structures, which could be present in multiple layers: subretinal, intraretinal and preretinal and across different locations in the retina (Table 1). For example, while a 2D view of the retina may show a bridging structure of a subretinal laser scar, visualization of the 3D volume reveals the relationship between the height, number of the connecting laser scar bridges and retinal attachments and contour (Fig.5). The appearance suggested that even with retinal detachment present, the laser scars may limit extension or height of subretinal fluid.

Next, we considered the visualization of such structures as they change during surgical maneuvers and interaction with instruments in surgery for complications of PDR. As detailed in all of the figures, the benefit of 3D visualization of complex structures and their orientation becomes even more important as these dynamically change during the course of surgery (4D viewing). 4D viewing gives the surgeon a better orientation and understanding of these specific pathologic structures in relation to adjacent tissue and instruments. This 4D view is essential as adjacent structures may be actively deforming as the instruments are moving.

While both 2D and 4D SS-MIOCT feedback were useful for assessing posterior pole membranes and macular contour after vitreous hemorrhage removal, the 4D viewing of actively changing structures during surgery for PDR facilitated intraoperative decision making throughout the surgical approach. During surgical maneuvers, visualization of the dynamic instrument-tissue interaction could be difficult using the 2D (B-scan) only. The 2D

(B-scan) shows a portion of the instrument or tissue of interest within the B-scan plane, which makes it difficult to track this dynamic interaction. 4D imaging by SS-MIOCT can facilitate visualization of this dynamic interaction through revealing the 3D structure of an instrument tip or membrane of interest relative to the retina. Thus throughout the surgery, feedback from the SS-MIOCT informed the surgeon as one progressed from one area of pathology to the next. Moreover, volume rotation via the surgeon-controlled joystick could provide more details through viewing this dynamic interaction between the instruments and membranes from different angles.

One example of SS-MIOCT feedback during numerous surgical steps was the use of intraoperative OCT in a case of viscodissection of a dense sheet of fibrovascular membranes with TRD. SS-MIOCT provided the surgeon with an important guidance during viscodissection through confirming when a full thickness hole had been created in the proliferative tissue before injecting viscoelastic. Furthermore, through volume rotation, the surgeon was able to see both the surface and undersurface of the fibrovascular membrane, its separation from the retina during excision, and the location of openings in the preretinal tissue. This dynamic imaging information has the potential to give the surgeons a whole new view to the tissue of interest.

While the study shows promising and new results for the use of intraoperative SS-MIOCT in surgery for complications of PDR, it has many limitations. We demonstrated the limited utility of SS-MIOCT in four cases of surgery with high TRD. In these cases, while MIOCT images were captured (Fig.1), retina and pre-retinal tissue could not be readily distinguished and this was confounded by tissue extending outside of the field of view. In contrast to other MIOCT studies which included a wide

range of vitreoretinal conditions, we included only diabetic cases which are characterized by the complexity of pathologies. Another limitation is the small number of cases across a range of complexity, which therefore did not allow for a statistical analysis of our study results. Despite the unique information, the SS-MIOCT device also showed multiple limitations. While 4D scans give better appreciation of the whole area of interest, the small field of view, limited depth of field and slow refresh rate of the current generation of the research SS-MIOCT system still limits the utmost benefit from this technology. Together, these made it difficult to maintain an OCT view during a rapid shift of focus or rapid surgeon movement. This was particularly evident in high TRD cases. The slow refresh rate also limited tracking the surgical tool if moved quickly across the retinal surface.

While the multiple artifacts described in the results impacted the optimal visualization using SS-MIOCT, identification of these artifacts was important for proper image analysis and for avoiding any misleading feedback during surgery or postoperative review. Further research is currently ongoing to limit the appearance of these artifacts. In most cases, simultaneous recording of the conventional microscope view with the corresponding intraoperative OCT imaging was not technically possible. This technical issue created a challenge in matching the two recordings for postoperative review. Although the volume rotation within the HUD could provide additional guidance to the surgeon, it also raises the problem of giving too much input to the surgeon during surgery. Within the microscope oculars, the surgeon can see 3 different views for the same area of interest, which are the conventional microscope view, 2D B-scans and 3D OCT scans in addition to the ability of volume rotations which can give different angles of view for the same area. Intraoperative interpretation

of all these information could be challenging for the surgeon especially while performing surgical maneuvers. Further advances are needed to find a more surgeon-friendly interface for intraoperative image viewing.

In this study, we demonstrated the utility and feasibility of intraoperative SS-MIOCT in the complex surgeries for PDR complications. We showed different scenarios during the surgery where the use of this technology can impact surgical decision making and guide surgical steps. We also suggested that intraoperative live volumetric (4D) visualization can provide important input not only about the retinal surface and the overlying membranes, but also about the subsurface of these tissues. With the advances in the 3D retina surgery using a large external heads up display²², integration of our 4D intraoperative OCT system into this technology could be the foundation of a new era in vitreoretinal surgery. This study identified areas important for future research including visualization and tracking of instrumentation, and methods to improve the speed of capture and field of view of intraoperative OCT images.

REFERENCES

1. Newman DK. Surgical management of the late complications of proliferative diabetic retinopathy. *Eye*. 2010;24(3):441-449.
2. Sharma S MT, Hariprasad SM. Surgical management of proliferative diabetic retinopathy. *Ophthalmic Surgery, Lasers & Imaging Retina*. 2014;45(3):188-193.
3. Hahn P, Migacz J, O'Connell R, Izatt JA, Toth CA. Unprocessed real-time imaging of vitreoretinal surgical maneuvers using a microscope-integrated spectral-domain optical coherence tomography system. *Graefe's archive for clinical and experimental ophthalmology = Albrecht von Graefes Archiv fur klinische und experimentelle Ophthalmologie*. 2013; 251 (1): 213-220.
4. Rabinowitz R, Yagev R, Shoham A, Lifshitz T. Comparison between clinical and ultrasound findings in patients with vitreous hemorrhage. *Eye (London, England)*. 2004;18(3):253-256.
5. Genovesi-Ebert F, Rizzo S, Chiellini S, Di Bartolo E, Marabotti A, Nardi M. Reliability of standardized echography before vitreoretinal surgery for proliferative diabetic retinopathy. *Ophthalmologica Journal internationale d'ophtalmologie International journal of ophthalmology Zeitschrift fur Augenheilkunde*. 1998;212 Suppl 1:91-92.
6. Silverman RH. Focused ultrasound in ophthalmology. *Clinical Ophthalmology (Auckland, NZ)*. 2016;10:1865-1875.
7. Ehlers JP, Xu D, Kaiser PK, Singh RP, Srivastava SK. Intraoperative dynamics of macular hole surgery: an assessment of surgery-induced ultrastructural alterations with intraoperative optical coherence tomography. *Retina (Philadelphia, Pa)*. 2014;34(2):213-221.
8. Ehlers JP, Tam T, Kaiser PK, Martin DF, Smith GM, Srivastava SK. Utility of Intraoperative Optical Coherence Tomography During Vitrectomy Surgery for Vitreomacular Traction Syndrome. *Retina (Philadelphia, Pa)*. 2014; 34 (7): 1341-1346.
9. Ehlers JP, Ohr MP, Kaiser PK, Srivastava SK. Novel microarchitectural dynamics in rhegmatogenous retinal detachments identified with intraoperative optical coherence tomography. *Retina (Philadelphia, Pa)*. 2013;33(7):1428-1434.
10. Ehlers JP, Goshe J, Dupps WJ, et al. Determination of Feasibility and Utility of Microscope-integrated OCT During Ophthalmic Surgery: the DISCOVER Study RESCAN Results. *JAMA ophthalmology*. 2015;133(10):1124-1132.
11. Ehlers JP, Tao YK, Srivastava SK. The Value of Intraoperative OCT Imaging in Vitreoretinal Surgery. *Current opinion in ophthalmology*. 2014;25(3):221-227.
12. Falkner-Radler CI, Glittenberg C, Gabriel M, Binder S. Intraoperative microscope-integrated spectral domain optical coherence tomography-assisted membrane

- peeling. *Retina (Philadelphia, Pa)*. 2015;35(10):2100-2106.
13. Ray R, Baranano DE, Fortun JA, et al. Intraoperative microscope-mounted spectral domain optical coherence tomography for evaluation of retinal anatomy during macular surgery. *Ophthalmology*. 2011; 118 (11): 2212-2217.
 14. Wykoff CC, Berrocal AM, Scheffler AC, Uhlhorn SR, Ruggeri M, Hess D. Intraoperative OCT of a full-thickness macular hole before and after internal limiting membrane peeling. *Ophthalmic surgery, lasers & imaging : the official journal of the International Society for Imaging in the Eye*. 2010; 41(1):7-11.
 15. Binder S, Falkner-Radler CI, Hauger C, Matz H, Glittenberg C. Feasibility of intrasurgical spectral-domain optical coherence tomography. *Retina (Philadelphia, Pa)*. 2011; 31 (7):1332-1336.
 16. Carrasco-Zevallos OM, Keller B, Viehland C, et al. Optical Coherence Tomography for Retinal Surgery: Perioperative Analysis to Real-Time Four-Dimensional Image-Guided Surgery Evolution of OCT for Retinal Surgery. *Investigative Ophthalmology & Visual Science*. 2016; 57(9):OCT37-OCT50.
 17. Carrasco-Zevallos OM, Keller B, Viehland C, et al. Live volumetric (4D) visualization and guidance of in vivo human ophthalmic surgery with intraoperative optical coherence tomography. *Scientific Reports*. 2016;6:31689.
 18. Shen L, Carrasco-Zevallos O, Keller B, et al. Novel microscope-integrated stereoscopic heads-up display for intrasurgical optical coherence tomography. *Biomedical optics express*. 2016;7(5):1711-1726.
 19. Iwasaki T, Miura M, Matsushima C, Yamanari M, Makita S, Yasuno Y. Three-dimensional optical coherence tomography of proliferative diabetic retinopathy. *The British journal of ophthalmology*. 2008; 92 (5):713.
 20. Dayani PN, Maldonado R, Farsiu S, Toth CA. Intraoperative use of handheld spectral domain optical coherence tomography imaging in macular surgery. *Retina (Philadelphia, Pa)*. 2009;29(10):1457-1468.
 21. Ehlers JP. Intraoperative OCT during Vitreoretinal Surgery for Dense Vitreous Hemorrhage in the PIONEER Study. 2015; 35(12):2537-2542.
 22. Eckardt C, Paulo EB. heads-up surgery for vitreoretinal procedures: An Experimental and Clinical Study. *Retina (Philadelphia, Pa)*. 2016;36(1):137-147.

دراسة دور التصوير الطبي المقطعي اثناء عمليات ازالة الجسم الزجاجي

البيانات الخلفية : يعتبر التصوير الطبي المقطعي اثناء عمليات الجسم الزجاجي من التقنيات الحديثة نسبيًا و التي تساعد علي امداد الجراحين بمعلومات مهمة عن طبقات الشبكية المختلفة و التغيرات التي تحدث لهذه الطبقات اثناء اجراء الجراحة. لقد اظهرت العديد من الدراسات فوائد هذه التقنية الحديثة اثناء عمليات الشبكية المختلفة و كيف ان الصور و المعلومات التي يتم الحصول عليها اثناء العملية عن طريق هذه التقنية تساعد الجراح علي اتخاذ الكثير من القرارات المهمة اثناء العملية.

الغرض : تقييم تقنية التصوير الطبي المقطعي اثناء اجراء جراحات الجسم الزجاجي لمضاعفات الاعتلال السكري لشبكية العين

المرضي و الطرق : تناول هذا البحث علاج ٢٠ مريض بمضاعفات الاعتلال السكري لشبكية العين عن طريق عمليات ازالة الجسم الزجاجي و بمساعدة تقنية التصوير الطبي المقطعي اثناء الجراحة و التي تمت عن طريق جهاز بحثي تجريبي يستخدم تقنية التصوير الطبي المقطعي رباعي الابعاد.

النتائج : اظهرت النتائج نجاح جهاز التصوير الطبي المقطعي رباعي الابعاد في التقاط صور ذات جودة جيدة في ١٦ حالة من اصل ٢٠ حالة. في هذه الحالات تمكن الجهاز من التقاط صور لمختلف الاعتلالات الشبكية المصاحبة لمرض السكري. ايضا ساعد الجهاز الجراح اثناء ازالة تليفات الشبكية عن طريق التقاط صور لاماكن هذه التليفات و مساعدة الجراح علي ايجاد البقعة المناسبة ليبدأ منها عملية ازالة التليفات من سطح الشبكية بدون التسبب في اضرار شبكية العين. في ٤ حالات من اصل ٢٠ حالة كانت الصور منخفضة الجودة و لم تضيف الكثير من المعلومات للجراح.

الاستنتاج : ان جهاز التصوير الطبي المقطعي رباعي الابعاد قادر علي تزويد الجراح بمعلومات و ارشادات مناسبة اثناء عمليات الجسم الزجاجي لمرضي مضاعفات الاعتلال الشبكي المصاحب لمرض السكري مما يساعد الجراح علي اتخاذ قرارات سليمة اثناء